PCCP

Cite this: *Phys. Chem. Chem. Phys.*, 2011, **13**, 7997–8007

www.rsc.org/pccp

PAPER

Kinetic studies on the temperature dependence of the BrO + BrO reaction using laser flash photolysis

Valerio Ferracci, Kaori Hino and David M. Rowley*

Received 10th December 2010, Accepted 4th March 2011
DOI: 10.1039/c0cp02847a

The BrO self-reaction, BrO + BrO → products (1), has been studied using laser flash photolysis coupled with UV absorption spectroscopy over the temperature range T = 266.5–321.6 K, under atmospheric pressure. BrO radicals were generated *via* laser photolysis of Br_2 in the presence of excess ozone. Both BrO and O_3 were monitored *via* UV absorption spectroscopy using charge-coupled device (CCD) detection. Simultaneous fitting to both temporal concentration traces allowed determination of the rate constant of the two channels of reaction (1), BrO + BrO → 2Br + O_2 (1a); BrO + BrO → Br_2 + O_2 (1b), hence the calculation of the overall rate of reaction (1) and the branching ratio, α: k_{1a}/cm^3 molecule^{-1} s^{-1} = (1.92 ± 1.54) × 10^{-12} exp[(126 ± 214)/T], k_{1b}/cm^3 molecule^{-1} s^{-1} = (3.4 ± 0.8) × 10^{-13} exp[(181 ± 70)/T], k_1/cm^3 molecule^{-1} s^{-1} = (2.3 ± 1.5) × 10^{-12} exp(134 ± 185 /T) and $\alpha = k_{1a}/k_1$ = (0.84 ± 0.09) exp[(−7 ± 32)/T]. Errors are 1σ, statistical only. Results from this work show a weaker temperature dependence of the branching ratio for channel (1a) than that found in previous work, leading to values of α at temperatures typical of the Polar Boundary Layer higher than those reported by previous studies. This implies a shift of the partitioning between the two channels of the BrO self-reaction towards the bromine atom and hence directly ozone-depleting channel (1a).

1. Introduction

Characterising the reactivity of bromine monoxide radicals, BrO, is of crucial importance to understand recent changes in the Earth's atmosphere. BrO radicals play a critical role in ozone-depleting events, both in Polar Regions and at midlatitudes. In the stratosphere, for instance, the BrO + ClO cycle is one of the major contributors to catalytic ozone destruction observed during Polar Springtime.[1] In the troposphere, ozone depletion has been detected in the Arctic Marine Boundary Layer and has been associated with enhanced BrO mixing ratios.[2,3]

Many studies have shone light on the origins and chemistry of atmospheric bromine. It is now known that, whilst the vast majority of atmospheric chlorine originates from anthropogenic sources, a considerable part of bromine present in the atmosphere is emitted by biogenic sources, such as phytoplankton. Moreover, despite the lower atmospheric abundance of bromine compared to chlorine,[4] bromine-driven ozone destruction is more efficient on a per atom basis as the active forms of bromine, Br and BrO, are more thermodynamically and photolytically preferred to their reservoir (inactive) forms compared to their chlorine counterparts.[5,6] The BrO self-reaction occurs at suitably high BrO mixing ratios. The current understanding of this reaction is that it comprises of two channels:[7,8]

$$BrO + BrO \rightarrow 2Br + O_2 \quad (1a)$$

$$\rightarrow Br_2 + O_2 \quad (1b)$$

At ambient temperature the reaction is dominated by channel (1a), which, in the presence of ozone, leads to ozone removal *via* reaction (2):

$$Br + O_3 \rightarrow BrO + O_2 \quad (2)$$

Therefore, for every Br atom produced by channel (1a), one ozone molecule is consumed by reaction (2), which in turn catalytically regenerates BrO. The BrO self-reaction is therefore not only atmospherically important as a key step in its own right as a catalytic ozone-depleting cycle, but it must be also taken into account when studying, in the laboratory, other atmospherically important reactions such as BrO + HO_2 and BrO + ClO.

A number of studies have focused on the BrO self-reaction[5,7–21] using a variety of techniques, from temperatures as low as T = 202 K[19] up to T = 573 K.[9] Most studies are in relatively good agreement at T = 298 K, and their results at ambient temperature are summarised in Table 1. Some studies[5,7,8,12,13,16,19,21] have investigated the temperature dependence of the BrO self-reaction: the majority of these observed a negative temperature

Department of Chemistry, University College London, Christopher Ingold Laboratories, 20 Gordon Street, London WC1H 0AJ, UK. E-mail: d.m.rowley@ucl.ac.uk

Table 1 Summary of previous studies on the kinetics of the BrO self-reaction

Reference	Technique[a]	T/K	p/Torr	$k_1(T = 298\ \mathrm{K})/10^{-12}$ cm^3 molecule^{-1} s^{-1}	$k_{1a}(T = 298\ \mathrm{K})/10^{-12}$ cm^3 molecule^{-1} s^{-1}	$k_{1b}(T = 298\ \mathrm{K})/10^{-13}$ cm^3 molecule^{-1} s^{-1}	$\alpha\ (T = 298\ \mathrm{K}) = k_{1a}/k_1$
Clyne and Cruse[9]	DF/UV	293–573	1	5.2 ± 0.6			
Basco and Dogra[10]	FP/UV	298	400–760	1.1 ± 0.2			
Clyne and Watson[11]	DF/MS	298		3.2 ± 0.7			
Jaffe and Mainquist[7]	PD	258–333					0.84 ± 0.01
Sander and Watson[8]	FP/UV	223–	50–475	2.17 ± 0.68		3.46 ± 0.68[b]	0.84 ± 0.3[b]
						4.12 ± 1.99[b]	0.81 ± 0.46[b]
Cox *et al.*[12]	MM/UV	278–338				6.9 ± 1.4[c]	0.84 ± 0.5[c]
Turnipseed *et al.*[13]	DF/MS	253–400	2	2.45 ± 0.26[d]			0.88 ± 0.04[d]
Lançar *et al.*[14]	DF/MS	298	1–2	3.2 ± 0.5	2.7 ± 0.5	4.7 ± 1.5	0.85 ± 0.3
Bridier *et al.*[15]	FP/UV	298	760	3.1 ± 0.4[e]		4.9 ± 0.6	
Mauldin *et al.*[5]	FP/UV	220, 298	75–600	2.7 ± 0.5	2.3 ± 0.3	4.4 ± 0.8	0.84 ± 0.01[f]
Rattigan *et al.*[16]	CP/UV	298–343	343–647			3.38 ± 0.33	
Rowley *et al.*[17]	FP/UV	298	760	2.98 ± 0.42	2.42 ± 0.42	4.69 ± 0.68	0.85 ± 0.03
Laszlo *et al.*[18]	LP/UV	295	200	2.8 ± 0.5[g]			
Gilles *et al.*[19]	LP/UV	204–388	500	3.5 ± 0.35			
Bedjanian *et al.*[20]	DF/MS	298	1	2.75 ± 0.35	2.35 ± 0.4	4.0 ± 0.5	0.84 ± 0.03[f]
Harwood *et al.*[21]	FP-LP/UV	222–298	100–760	2.90 ± 0.28	2.59 ± 0.28	3.1 ± 0.2	0.89 ± 0.13
IUPAC[22]				3.2 ± 0.3	2.7 ± 0.3	4.8 ± 0.5	0.85 ± 0.11
JPL-NASA[23]				3.25	2.74	5.02	0.84
This work	LP/UV	265–320	760	3.4 ± 0.08	2.8 ± 0.08	5.75 ± 0.07	0.83 ± 0.03

[a] DF/UV = discharge flow/UV absorption spectroscopy; FP/UV = flashlamp photolysis/ UV absorption spectroscopy; DF/MS = discharge flow/mass spectrometry; PD = photosensitised decomposition; MM/UV = molecular modulation/UV spectroscopy; CP/UV = continuous photolysis/ UV absorption spectroscopy; LP/UV = laser photolysis/ UV absorption spectroscopy. [b] Sander and Watson used two different methods to measure k_{1b}. The first consisted in monitoring BrO decay in excess O_3. The second involved measurements of the quantum yield of O_3 loss. [c] At $T = 303$ K. [d] At $T = 304$ K. [e] Calculated assuming $\alpha = 0.84$. [f] Error as reported by the authors. [g] At $T = 295$ K.

dependence for the overall rate constant and for channel (1b) along with a weaker, near-zero temperature dependence for channel (1a). However these studies have reported somewhat conflicting results with regard to the absolute values of the individual rate constants. The work of Sander and Watson[8] was the first to investigate the overall rate of reaction (1) at temperatures other than $T = 298$ K; these authors measured k_1 at three temperatures over the range $T = 223$–338 K. Cox *et al.*[12] reported values for k_{1b} and for the branching ratio $\alpha = k_{1a}/k_1$ at four temperatures over the range $T = 278$–338 K and found greater rate constants than those reported by Sander and Watson as well as a weaker negative temperature dependence for k_{1b}. However, measurements of k_1 by Turnipseed *et al.*[13] at three temperatures over the range $T = 253$–400 K showed good agreement with the work of Sander and Watson. Mauldin *et al.*[5] determined the rate constants of both channels, hence the overall rate constant and the branching ratio, at $T = 298$ K and $T = 220$ K. Gilles *et al.*[19] measured k_1 at nine temperatures over the range $T = 204$–388 K, finding values of the overall rate constant higher than those of Sander and Watson[8] and Turnispeed *et al.*[13] Harwood *et al.*[21] measured k_{1a} and k_{1b} at five temperatures over the range $T = 222$–298 K, and obtained smaller rate constants than previous work. A more in-depth account of previous studies on the BrO self-reaction is presented in section 4.1 below.

Studies on the BrO self-reaction at low temperatures are complicated by the contribution of a termolecular component to the observed BrO decay at $T < 250$ K, as reported by Mauldin *et al.*[5] and Harwood *et al.*[21] Both studies found that the overall rate constant was pressure-dependent at $T = 220$ K and $T = 222$ K respectively and reported an additional absorption in their spectra attributed to the BrO dimer. However, Sander and Watson reported pressure-independent values of k_1 at a similar temperature ($T = 223$ K). In addition, most studies on the temperature dependence of the BrO self-reaction carry significant statistical uncertainties as measurements are only available at a small number of temperature points (with the exception of the work of Gilles *et al.*[19]).

JPL-NASA recommendations[23] for the BrO self-reaction have remained unchanged since 1997. The recommended temperature dependence for the overall rate constant of reaction (1), k_1, is based on the work of Sander and Watson,[8] Turnipseed *et al.*[13] and Gilles *et al.*,[19] whereas the temperature dependence of the branching ratio α is based on the study by Mauldin *et al.*[5] (who measured the branching ratio only at two temperatures, $T = 298$ K and 220 K) and on an extrapolation of the data from Cox *et al.*,[12] who measured the branching ratio only down to $T = 277.5$ K, to lower temperatures. Extrapolation of the data from Cox *et al.* to $T = 220$ K gives a value of α of 0.72, whereas Mauldin *et al.* measured a branching ratio of 0.68 at this temperature. It appears therefore that the branching of the two channels, whilst well-established at ambient temperature, is still poorly characterised at sub-ambient temperatures relevant to the Arctic Boundary Layer, due to the paucity of studies performed at such temperatures.

This study aimed to measure the rate constants of both channels of the BrO self-reaction at sub-ambient temperatures (down to $T = 266.5$ K) and to accurately characterise the temperature dependence of the branching ratio employing laser flash photolysis coupled with UV absorption spectroscopy. Many previous studies have employed this technique, most of them using a flashlamp as the source of photolysis,[5,8,10,15,17] others using a laser.[18,19,21] However the present study is the first to combine the advantages of laser photolysis (selective photolysis of precursor gases, reduced undesired secondary chemistry, reduced experimental noise) with those of CCD

detection (*i.e.* simultaneous spectral and temporal resolution of recorded UV absorbances).

2. Experimental

The kinetics of the BrO self-reaction were studied by means of laser flash photolysis coupled with time-resolved broadband UV absorption spectroscopy with charge coupled device (CCD) detection. The apparatus has been already described extensively[17] hence only a brief summary is given here.

2.1 Gas handling

Gaseous $Br_2/O_3/O_2/N_2$ mixtures were prepared using calibrated mass flow controllers (MKS). Bromine vapour was introduced into the gas mixture by passing a small flow of nitrogen gas through a bubbler containing liquid Br_2 (Acros, 99.8%) kept at 0 °C inside a Dewar flask. The bromine content in the precursor mixture was calculated using the vapour pressure of liquid Br_2 at 0 °C and was typically (4–5) $\times$ 10^{16} molecules cm^{-3}. Ozone was generated by flowing oxygen (BOC, 99.99%) gas through a commercial ozoniser (Ozonia, Triogen). A separate set of experiments was undertaken to determine the conversion efficiency of the ozoniser: the O_3 output was measured *via* UV spectroscopy and quantified using the Beer–Lambert law (see section 3.1) and the JPL-NASA[23] recommended absorption cross-section. The typical conversion efficiency was found to be approximately 6% and ozone concentrations in the precursor mixture were (1–2) $\times$ 10^{16} molecules cm^{-3}. These gases were mixed with a nitrogen (BOC, 99.998%) bath gas to balance to p = 1 atm in a Pyrex mixing line from which they were delivered to the reaction cell *via* Teflon tubing. Gases flowed continuously through the cell (a cylindrical thermostatted quartz vessel 98.2 cm in length and 1.48 cm in diameter) so that a fresh mixture of precursor gases was present for each photolysis event. Gas flow-out from the reaction cell, a consequence of the continuous flow set-up, was taken into account in the analytical procedure and was in any way minimal over the timescale of the observed radical decay.

2.2 Radical generation

An excimer laser (Lambda Physik COMPex 201), operating at λ = 351 nm with typical output of approximately 110 mJ per pulse, was used to initiate the chemistry leading to the formation of BrO radicals. The laser beam was first expanded *via* a pair of fused silica cylindrical lenses, and then collimated through an iris to match the cross-sectional area of the reaction cell. A dichroic reflector directed the laser beam through the cell, in a direction opposite to that of the UV analysing light.

Chemistry following photolysis of $Br_2/O_3/O_2/N_2$ mixtures consisted of the reaction of the photolytically generated Br atoms with excess ozone to produce BrO:

$$Br_2 + h\nu\,(351\ nm) \rightarrow 2Br \qquad (3)$$

$$Br + O_3 \rightarrow BrO + O_2 \qquad (2)$$

The optimised experimental conditions minimised the occurrence of secondary chemistry such that BrO radicals were promptly and exclusively formed from Br atoms. Post-photolysis bromine atom concentrations, $[Br]_0$, and therefore initial BrO concentrations, $[BrO]_0$, were typically in the range (5–6) $\times$ 10^{13} molecules cm^{-3} and were determined from fits to the kinetic traces, as discussed below.

2.3 Radical monitoring

Species in the reaction mixture were monitored by UV absorption spectroscopy accompanied by CCD detection. Light from a 75 W continuous xenon arc lamp (Hamamatsu L2174) was collimated and passed once through the gaseous mixture. Light exiting the cell was focused onto the entrance slit of a 0.25 m astigmatic Czerny–Turner spectrograph (Chromex 250IS) equipped with a 600 grooves mm^{-1} diffraction grating. The width of the entrance slit was set to 75 μm for this work, resulting in a resolution (FWHM) of 0.5 nm and typically the window λ = 298–326 nm was monitored. Wavelength-resolved transmitted light was imaged onto the top 31 rows of the two-dimensional CCD detector. A more in-depth description of CCD detection can be found elsewhere.[17,21,24,25] The CCD detector enabled rapid and efficient transfer of light-generated signal out of the illuminated region of the detector in the axis perpendicular to the spectral axis. Hence the CCD array allowed acquisition of spectrally-resolved light intensities recorded sequentially before, during and after laser photolysis at a temporal resolution dictated by the time elapsed between each charge transfer in the CCD device (*shift time*). In this work, spectra were typically recorded at intervals of 100 μs.

3. Data analysis

3.1 Determination of absorbances and concentrations

Absorbance spectra were obtained from the recorded light intensities using Beer's Law:

$$A_{\lambda,t} = \ln\left(\frac{\langle I_{\lambda,\text{pre-flash}}\rangle}{I_{\lambda,t}}\right) \qquad \text{(i)}$$

where $A_{\lambda,t}$ is the absorbance at wavelength λ and time t, $\langle I_{\lambda,\text{pre-flash}}\rangle$ is the *average* light intensity at wavelength λ preceding photolysis and $I_{\lambda,t}$ is the light intensity at wavelength λ recorded at any time t. Therefore the absorbance spectra obtained represented the *change* in the total absorbance of the reactive mixture post-photolysis. A typical absorbance spectrum recorded in this study is shown in Fig. 1: the distinctive peaks arise from the ($A\ ^2\Pi_{3/2} \leftarrow X\ ^2\Pi_{3/2}$) vibronic transition of BrO, whilst the negative absorbance observed at shorter wavelengths is attributed to ozone removal *via* reaction (2).

The concentrations of the species of interest were determined using the Beer–Lambert Law:

$$A_{\lambda,t} = \sum_i \sigma_{i,\lambda} l [i]_t \qquad \text{(ii)}$$

where $\sigma_{i,\lambda}$ is the absorption cross-section of species i at wavelength λ, l is the optical pathlength of the analysis light through the reaction mixture and $[i]_t$ is the concentration of species i at time t. Concentrations were obtained by fitting reference cross-sections to the recorded absorbance. The BrO spectrum measured by Wilmouth *et al.*[6] was used as the reference BrO cross-section in this work. The resolution of

this spectrum was higher (0.4 nm FWHM) than that of the experimental spectra from this work (0.5 nm FWHM). Since the absorption cross-section of vibronic features of the BrO spectrum are a strong function of spectral resolution, the cross-section from Wilmouth *et al.* was smoothed using in this case a 93-point Gaussian averaging kernel to match the lower experimental resolution of the present work. The absence of systematic features in the residuals obtained from spectral subtraction of the scaled reference from the experimental spectra added confidence to this smoothing procedure, as shown in Fig. 1. The vibronic bands of BrO are also strongly dependent on temperature: reference BrO cross-sections were interpolated to each experimental temperature again using the spectra recorded by Wilmouth *et al.* at T = 228 K and T = 298 K, assuming that σ_{BrO} changed linearly with temperature over this range. At each temperature, the absence of any residual structure following spectral fitting and subtraction confirmed the determination of BrO concentrations.

The values for the ozone cross-section used to fit to eqn (ii) were those reported by JPL-NASA.[23] Unlike the BrO spectrum, ozone absorption in the near-UV at the current experimental resolution is devoid of significant structured features and therefore does not exhibit an appreciable dependence on spectral resolution. Smoothing of the ozone cross-section was not therefore required. Temperature effects on the ozone cross-section are also very weak: however, reference O_3 cross-sections were generated at each experimental temperature *via* an interpolation of the JPL-NASA temperature-dependent cross-section in a manner similar to that used for the BrO spectrum.

Differential fitting procedures were used to determine BrO concentrations. This technique has been described in detail elsewhere[24] and, by virtue of high-pass filtering to obtain the spectrally structured absorptions alone, allows unequivocal monitoring of such absorbers. Initially, differential fitting was used to quantify $[BrO]_t$ alone. As BrO was the only absorber with spectral structure present in the gas mixture post-photolysis, eqn (ii) was expressed as:

$$A_{\text{diff }\lambda,t} = \sigma_{\text{diff BrO},\lambda} l [BrO]_t \qquad \text{(iii)}$$

where $A_{\text{diff }\lambda,t}$ is the differential absorbance spectrum and $\sigma_{\text{diff BrO},\lambda}$ is the differential BrO cross-section. However, monitoring $[BrO]_t$ only is not sufficient to investigate both channels of reaction (1) (see section 3.2). To achieve a full kinetic characterisation of the BrO + BrO self-reaction it was also necessary to monitor the change in ozone concentration following photolysis, $\Delta[O_3]_t$. In direct (*i.e.* non-differential) absorption, eqn (ii) was therefore also expressed as

$$A_{\lambda,t} = l(\sigma_{BrO,\lambda}[BrO]_t + \sigma_{O_3,\lambda}\Delta[O_3]_t) \qquad \text{(iv)}$$

Typical $[BrO]_t$ and $\Delta[O_3]_t$ kinetic profiles obtained from fitting to eqn (iv) are shown in Fig. 2 and 3 respectively.

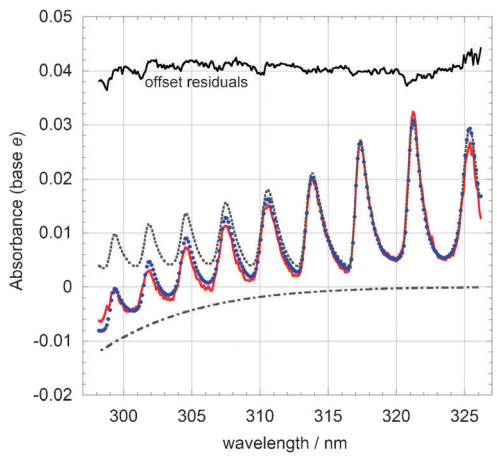

Fig. 1 Typical absorbance spectrum recorded at T = 265.5 K following photolysis of $Br_2/O_3/O_2/N_2$ gas mixtures (*in red*), showing the distinctive peaks arising from the A $^2\Pi_{3/2} \leftarrow$ X $^2\Pi_{3/2}$ vibronic transition of BrO and a negative contribution from ozone removal at shorter wavelengths. This spectrum was averaged over the first 50 ms after photolysis. Also shown are the contribution of BrO (*dotted line*) and ΔO_3 (*dot-dashed line*) to the total post-photolysis absorbance obtained from fitting reference cross-sections to the experimental spectrum, and the calculated absorbance resulting from the fit (*blue points*). Residuals are offset by +0.04 absorbance units for clarity.

3.2 Kinetic analysis

Experiments were performed under excess ozone such that Br atoms formed *via* channel (1a) reacted promptly with O_3 to regenerate BrO *via* reaction (2). Thus channel (1a) was effectively masked and the observed second-order BrO decay depended solely on k_{1b}. Using classical kinetics and assuming that Br atoms were in steady state (as confirmed by simulations using numerical integration), the rate of loss of BrO was written as:

$$-\frac{d[BrO]_t}{dt} = 2k_{1b}[BrO]^2 \qquad \text{(v)}$$

This equation is readily integrated to give an expression for the observed BrO decay:

$$[BrO]_t = \left(\frac{1}{[BrO]_0} + 2k_{1b}t\right)^{-1} \qquad \text{(vi)}$$

Thus, fitting a simulated [BrO] trace from eqn (vi) to the observed experimental BrO decay allowed extraction of the rate constant of channel (1b) but provided no kinetic information on channel (1a).

It was still however possible to measure k_{1a} by monitoring the change in ozone abundances after photolysis as discussed above. The rate of ozone removal *via* reaction (2) can be written as:

$$-\frac{d[O_3]_t}{dt} = k_2[Br][O_3] \qquad \text{(vii)}$$

Assuming that Br atoms are in steady state, it can be shown[8] that:

$$\Delta[O_3]_t = [O_3]_t - [O_3]_0 = -2k_{1a}[BrO]_0^2\left(\frac{t}{1 + 2k_{1b}t[BrO]_0}\right) \qquad \text{(viii)}$$

where $[O_3]_0$ is the concentration of ozone immediately following photolysis *and* generation of BrO radicals, and $[O_3]_t$ is the subsequent ozone concentration reduced further by the catalytic destruction of ozone following reaction (1a). Eqn (viii)

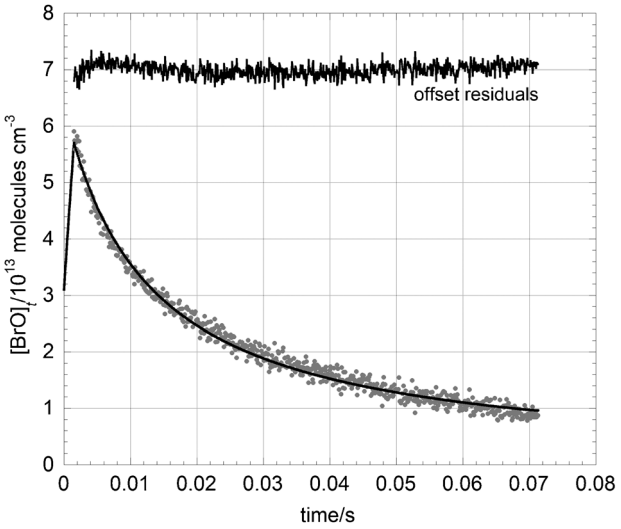

Fig. 2 Typical $[BrO]_t$ decay trace recorded at $T = 287.4$ K (*data points*). Also shown is the classical kinetic fit (*solid line*) to the experimental data. Residuals have been offset by $+7 \times 10^{13}$ molecules cm^{-3} for clarity.

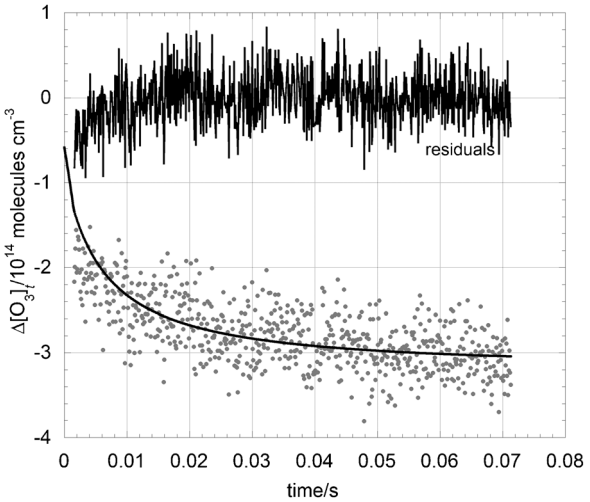

Fig. 3 Typical $\Delta[O_3]_t$ decay trace recorded at $T = 287.4$ K (*data points*). Also shown is the classical kinetic fit (*solid line*) to the experimental data.

therefore describes the temporal behaviour of $\Delta[O_3]$ without taking into account the ozone loss resulting from the initial formation of BrO *via* reaction (2). Assuming $[BrO]_0 = \Delta[O_3]_0$ from stoichiometry of BrO formation chemistry, eqn (viii) becomes:

$$\Delta[O_3]_t = -[BrO]_0\left\{2k_{1a}[BrO]_0\left(\frac{t}{1+2k_{1b}t[BrO]_0}\right)+1\right\} \quad \text{(ix)}$$

Eqn (viii) and (ix) show that ozone removal is sensitive to both k_{1a} and k_{1b} and hence allow the determination of the branching ratio of the BrO self-reaction, defined for channel (1a) as $\alpha = k_{1a}/k_1$.

Initially, eqn (vi) alone was fitted to the experimental $[BrO]_t$ trace *via* a least-squares minimisation routine optimising the values for $[BrO]_0$ and k_{1b}. Subsequently, eqn (vi) and (ix) were fitted *simultaneously* to the observed $[BrO]_t$ and $\Delta[O_3]_t$ traces respectively by optimising $[BrO]_0$, k_{1a} and k_{1b}. Typical kinetic fits to these traces are also shown in Fig. 2 and 3 along with offset residuals.

4. Results and discussion

4.1 Results

The BrO self-reaction was studied at nine temperatures over the range $T = 266.5$–321.6 K and at ambient pressure ($p = 760$ Torr). Typically at least four experiments were performed at each temperature, each consisting of 20 photolysis events. Two sets of data were obtained from the kinetic analysis (see section 3.2): one in which k_{1b} alone was extracted from the analysis of the BrO decay, and one in which both k_{1a} and k_{1b} were obtained from simultaneous fitting to $\Delta[O_3]_t$ and $[BrO]_t$. The kinetic parameters resulting from the two different fitting procedures are shown in Tables 2 and 3. The errors shown are 2σ, statistical only.

Both channels showed negative temperature dependence of the kinetic parameters and followed a linear Arrhenius behaviour. The Arrhenius expression for k_{1b} obtained from fitting solely to the observed BrO decay is:

$$k_{1b}/\text{cm}^3\ \text{molecule}^{-1}\ \text{s}^{-1} = (3.4 \pm 1.0) \times 10^{-13} \exp[(182 \pm 91)/T]$$

Simultaneous fitting to both $[BrO]_t$ and $[\Delta O_3]_t$ allowed characterisation of both channels as a function of temperature. The Arrhenius expressions resulting from this fitting procedure are:

$$k_{1a}/\text{cm}^3\ \text{molecule}^{-1}\ \text{s}^{-1} = (1.92 \pm 1.54) \times 10^{-12} \times \exp[(126 \pm 214)/T]$$

$$k_{1b}/\text{cm}^3\ \text{molecule}^{-1}\ \text{s}^{-1} = (3.4 \pm 0.8) \times 10^{-13} \exp[(181 \pm 70)/T]$$

Hence

$$k_1/\text{cm}^3\ \text{molecule}^{-1}\ \text{s}^{-1} = (2.3 \pm 1.5) \times 10^{-12} \exp(134 \pm 185/T)$$

cf. JPL-NASA:[23] $k_1 = 1.5 \times 10^{-12} \exp(230/T)$

Giving

$$\alpha = k_{1a}/k_1 = (0.84 \pm 0.09) \exp[(-7 \pm 32)/T]$$

cf. JPL-NASA:[23] $k_{1a}/k_1 = 1.6 \exp(-190/T)$

Arrhenius parameters (pre-exponential factor A and activation energy $-E_a/R$) are summarised in Table 4 along with the IUPAC[22] and JPL-NASA[23] recommendation and results from previous studies.

The two sets of results obtained for k_{1b} from different fitting methods are in excellent agreement with one another, with values of the rate constant at each temperature agreeing within error range (Tables 2 and 3). Consequently, the Arrhenius parameters for the temperature dependence of k_{1b} derived from the two independent analyses are analogous, implying that the sensitivity to k_{1b} from ozone traces gave identical values to those from BrO traces (Table 4). The consistency of

Table 2 Values for k_{1b} obtained from fitting to $[BrO]_t$ decay only. Errors are 2σ, statistical only

T/K	$k_{1b}/10^{-13}$ cm^3 molecule^{-1} s^{-1}
265.5	6.84 ± 0.08
272.5	6.62 ± 0.03
279.9	6.19 ± 0.16
287.4	6.14 ± 0.10
298	5.69 ± 0.09
302.4	5.95 ± 0.09
309.5	6.34 ± 0.11
315.5	6.26 ± 0.11
320.6	5.91 ± 0.08

the results for k_{1b} obtained from these two datasets added confidence to this work.

Arrhenius plots are shown in Fig. 4–6 for k_1, k_{1a} and k_{1b} respectively. The values plotted for k_{1b} are those from the simultaneous fit to $[BrO]_t$ and $[\Delta O_3]_t$. Comparison of the branching ratio α from this work with previous studies is shown in Fig. 7 and follows the convention used in JPL-NASA[23] of also describing the temperature dependence of the branching ratio in Arrhenius form.

4.2 Comparison with previous studies

Early studies on the BrO self-reaction[9–11] only focused on the overall rate of the reaction, $k_1 = k_{1a} + k_{1b}$. These results show poor agreement with one another, reflecting the uncertainties that were still surrounding the mechanism and products of the BrO self-reaction at the time. Jaffe and Mainquist[7] were the first to study the branching ratio $\alpha = k_{1a}/k_1$ by measuring the quantum yield of bromine photosensitised decomposition of ozone over the temperature range T = 258–333 K. They showed that channel (1a) was the dominating pathway over the experimental temperature range used, with a branching ratio of $\alpha = 0.84 \pm 0.01$ at T = 298 K. Sander and Watson[8] used flash photolysis coupled with UV absorption spectroscopy to measure k_1 at three temperatures (T = 223 K, 298 K and 388 K) and over the pressure range p = 50–475 Torr. A negative temperature dependence was reported for the overall reaction rate constant and no pressure dependence was observed at any of the temperatures used. k_{1b} was also measured at T = 298 K, thus allowing determination of the branching ratio at room temperature giving $\alpha = 0.84 \pm 0.3$, in excellent agreement with the findings of Jaffe and Manquist. Cox *et al.*[12] employed modulated photolysis coupled with UV absorption spectroscopy under excess ozone to monitor k_{1b} over the range T = 278–338 K. Greater rate constants than those reported by Sander and Watson were determined along with a weaker negative temperature dependence. The temperature dependence of the branching ratio was also obtained from analysis of the bromine sensitised decomposition of ozone and resulted in values of α ranging from 0.78 ± 0.03 at T = 277.5 K to 0.88 ± 0.01 at T = 348 K. Turnipseed *et al.*[13] carried out a study of the BrO self-reaction at low pressure (p = 2 Torr) using discharge flow coupled with mass spectrometry over the range T = 253–400 K, obtaining values of k_1 in good agreement with those of Sander and Watson. The same technique was used by Lançar *et al.*[14] to measure both k_1 and k_{1b} at T = 298 K, confirming the findings of Turnipseed *et al.* Bridier *et al.*[15] utilised flash photolysis coupled with UV absorption spectroscopy to monitor the rate of BrO decay through the self-reaction at T = 298 K. However the reaction conditions employed in their work (excess ozone) only allowed determination of k_{1b}, hence they inferred the total rate of reaction k_1 assuming $\alpha = 0.84$. The value obtained for k_1 was in good agreement with that reported by Lançar *et al.* but more than 40% higher than that of Sander and Watson, who used the same experimental technique. Mauldin *et al.*[5] measured the rate coefficients of both channels of the BrO self-reaction using flash photolysis coupled with UV absorption spectroscopy. k_{1a} and k_{1b} were determined at two temperatures, T = 220 K and 298 K, over the pressure range p = 75–600 Torr with a variety of bath gases (He, N_2 and SF_6). The overall rate coefficient k_1 was found to be independent of pressure at T = 298 K but dependent on pressure at T = 220 K. On the other hand, the branching ratio α was found to be independent of pressure at both temperatures and was found to be 0.84 ± 0.01 at T = 298 K and 0.68 ± 0.05 at T = 220 K. Rattigan *et al.*[16] used continuous photolysis with UV absorption spectroscopy, measuring k_{1b} over the temperature range T = 293–343 K. Their values are amongst the lowest to date and this is the only study indicating a positive temperature dependence for channel (1b). Rowley *et al.*[17] employed flash photolysis with the inclusion, for the first time in a gas kinetics study, of a two-dimensional charge-coupled device (CCD) detector for monitoring both wavelength and time resolved absorptions. The rate constants obtained in their work agree well with the studies of Mauldin *et al.*[5] and of Lançar *et al.*[14] Both Laszlo *et al.*[18] and Bedjanian *et al.*[20] studied the BrO self-reaction at ambient temperature, the first using laser flash photolysis with UV absorption spectroscopy, the second employing discharge flow coupled with mass spectrometry.

Table 3 Kinetic results from simultaneous fitting to both $[BrO]_t$ and $\Delta[O_3]_t$ traces. Errors are 2σ, statistical only

T/K	$k_{1a}/10^{-12}$ cm^3 molecule^{-1} s^{-1}	$k_{1b}/10^{-13}$ cm^3 molecule^{-1} s^{-1}	$k_1/10^{-12}$ cm^3 molecule^{-1} s^{-1}	k_{1a}/k_1
265.5	3.14 ± 0.3	6.93 ± 0.1	3.83 ± 0.3	0.82 ± 0.01
272.5	3.22 ± 0.3	6.73 ± 0.04	3.90 ± 0.3	0.83 ± 0.01
279.9	2.99 ± 0.33	6.29 ± 0.02	3.62 ± 0.3	0.82 ± 0.02
287.4	3.00 ± 0.2	6.21 ± 0.1	3.62 ± 0.2	0.83 ± 0.007
298	2.81 ± 0.09	5.75 ± 0.07	3.39 ± 0.08	0.83 ± 0.005
302.4	2.32 ± 0.4	6.03 ± 0.1	2.92 ± 0.4	0.79 ± 0.02
309.5	3.30 ± 0.6	6.40 ± 0.2	3.94 ± 0.6	0.83 ± 0.02
315.5	3.56 ± 0.4	6.30 ± 0.2	4.20 ± 0.4	0.85 ± 0.01
320.6	2.55 ± 0.5	5.91 ± 0.1	3.14 ± 0.5	0.81 ± 0.03

Table 4 Arrhenius parameters

	k_{1a}		k_{1b}	
	$A/10^{-12}$ cm^3 molecule^{-1} s^{-1}	$-E_a/R$/K	$A/10^{-14}$ cm^3 molecule^{-1} s^{-1}	$-E_a/R$ /K
JPL-NASA[23]	2.4	40	2.8	860
IUPAC[22]	2.7	0 ± 200	2.9	840 ± 200
Harwood *et al.*[21]	5.31 ± 1.17	211 ± 59	1.13 ± 0.47	983 ± 111
Cox *et al.*[12]			29^{+28}_{-14}	259 ± 208
This work (fit to $[BrO]_t$ alone)			34 ± 10	182 ± 91
This work (simultaneous fit to $[BrO]_t$ and $\Delta[O_3]_t$)	1.92 ± 1.54	126 ± 214	34 ± 8	181 ± 70

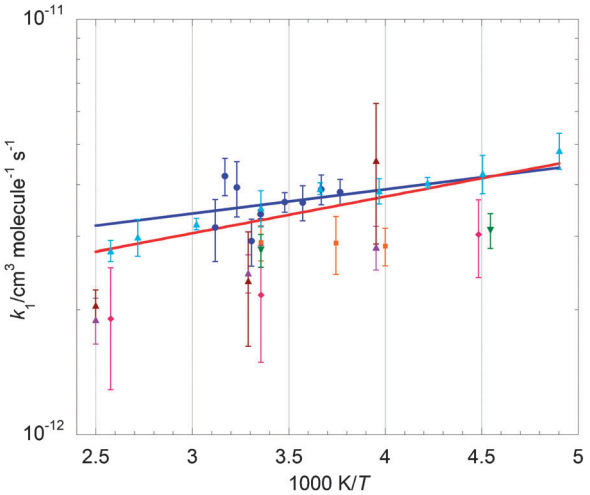

Fig. 4 Arrhenius plot for k_1 ($k_1 = k_{1a} + k_{1b}$): this work (blue circles and blue linear fit), Harwood *et al.*[21] (orange squares), Turnipseed *et al.*[13] using O + Br_2 (brown triangles), Turnipseed *et al.* using Br + O_3[13] (purple triangles), Sander *et al.*[8] (pink diamonds), Mauldin *et al.*[5] (green inverted triangles), Gilles *et al.*[19] (light-blue triangles) along with JPL-NASA recommendation[23] (red line). Errors from Harwood *et al.* are 1σ, as stated by the authors. Errors from this work are 2σ, statistical only.

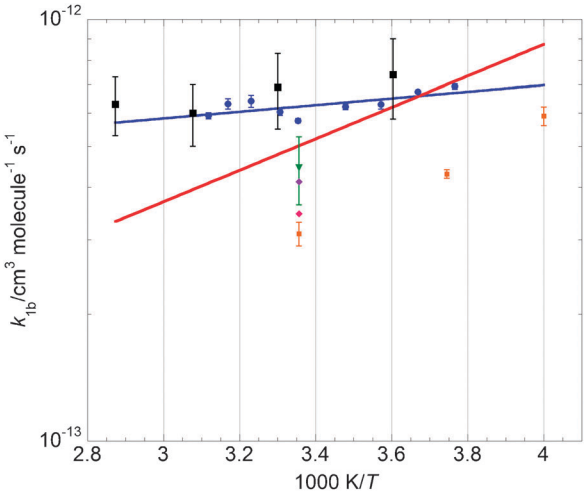

Fig. 6 Arrhenius plot for k_{1b}: this work (blue circles and blue linear fit), Harwood *et al.*[21] (orange squares), Sander and Watson from measurement of second-order BrO decay[8] (pink diamonds), Sander and Watson from measurement of quantum yield of O_3 destruction[8] (purple triangle), Cox *et al.*[12] (black squares), Mauldin *et al.*[5] (green inverted triangles) along with JPL-NASA recommendation[23] (red line). Errors from Harwood *et al.* are 1σ, as stated by the authors. Errors from this work are 2σ, statistical only.

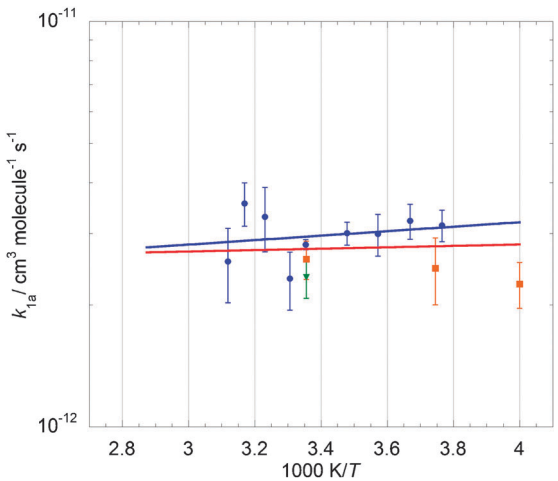

Fig. 5 Arrhenius plot for k_{1a}: this work (blue circles and blue linear fit), Harwood *et al.*[21] (orange squares), Mauldin *et al.*[5] (green inverted triangles) along with JPL-NASA recommendation[23] (red line). Errors from Harwood *et al.* are 1σ, as stated by the authors. Errors from this work are 2σ, statistical only.

Their findings are in good agreement with previous work. Gilles *et al.*[19] used laser photolysis coupled with UV absorption spectroscopy to measure the overall rate constant k_1 over the temperature range T = 204–388 K and at pressures p = 6–15 Torr. A negative temperature dependence for k_1 was observed, with higher values of the rate constant than those of Sander and Watson and Turnipseed *et al.* The study by Harwood *et al.*[21] is the most extensive to date, considering the temperature (T = 222–298 K) and pressure (p = 100–760 Torr) ranges over which the BrO self-reaction was characterised. Similarly to the work of Rowley *et al.*, flash photolysis with UV absorption spectroscopy using CCD detection was used to measure the rate constants of both channels. A negative temperature dependence of the rate constants was observed throughout, in agreement with almost all previous work. In addition, the overall rate coefficient k_1 was found to be dependent on pressure at temperatures below T = 250 K. This finding disagrees with Sander and Watson, who observed no pressure dependence at T = 223 K but agrees with Mauldin *et al.*, who reported a pressure-dependent k_1 at T = 220 K.

The overall rate constant of the BrO self-reaction, k_1, from this work is in good agreement with the findings of Gilles *et al.*[19] Unsurprisingly, the current JPL-NASA recommendation[23] (partly based on the work of Gilles *et al.*—see Introduction) lies within the error range at most experimental temperatures but

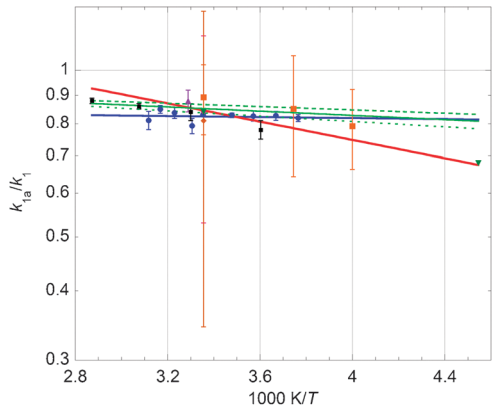

Fig. 7 Branching ratio for channel (1a) as a function of temperature: this work (blue circles and blue linear fit), Harwood *et al.*[21] (orange squares), Turnipseed *et al.*[13] (purple triangles), Sander and Watson from measurement of second-order BrO decay[8] (pink diamonds), Sander and Watson from measurement of quantum yield of O_3 destruction[8] (purple triangle), Cox *et al.*[12] (black squares), Jaffe and Mainquist[7] (bright green solid line with upper and lower uncertainty limits in bright green dashed lines) Mauldin *et al.* (green inverted triangles) along with JPL-NASA recommendation[23] (red line). Errors from this work are 2σ, statistical only.

does exhibit a stronger temperature dependence which becomes more evident at higher temperatures. However, extrapolation of data from this work to temperatures more relevant to Polar Regions is in relatively good agreement with the JPL-NASA evaluation.

On the other hand, the values obtained for the rate constant of channel (1a), k_{1a}, in this work show a slightly more pronounced temperature dependence than that reported in the current JPL-NASA evaluation.[23] The parameterisation from the present work suggests larger values of k_{1a} at low temperatures: extrapolation of our data to $T = 250$ K results in k_{1a} 13% higher than JPL-NASA and 42% higher than Harwood *et al.*[21] The divergence between the two temperature dependences becomes more manifest at $T = 220$ K, where extrapolation of data from the present work is approximately 20% higher than JPL-NASA recommendation. The scatter of the points in the Arrhenius plot for k_{1a} arises principally from the lower signal-to-noise ratio of the ozone kinetic traces, compared to those for BrO. However results from this study lie within current JPL-NASA uncertainty limits.

The temperature dependence of k_{1b} obtained in this study is in very good agreement with that of Cox *et al.*[12] but it is noticeably weaker than both the JPL-NASA recommendation and previous work from Sander and Watson,[8] Mauldin *et al.*[5] and Harwood *et al.*[21] Over the relatively narrow experimental range used in this work (of about 55 K), values of k_{1b} vary by a factor of 1.1 whereas the JPL-NASA recommended values vary by a factor of 1.7. The JPL-NASA recommended value for k_{1b} at $T = 250$ K is 25% greater than the value extrapolated from this work.

Unsurprisingly, as the k_{1a} measured in this work is greater than the JPL-NASA recommendation at low temperatures and k_{1b} has a much weaker negative temperature dependence than that evaluated by JPL-NASA, the branching ratio from this work reflects a net dominance of channel (1a) over channel (1b) not only at ambient temperature, but also at temperatures typical of Arctic Boundary Layer. The JPL-NASA recommendation is based on data from Cox *et al.*[12] and Mauldin *et al.*;[5] the evaluation for α is 0.84 at $T = 298$ K and 0.68 at $T = 220$ K. Most studies, including the present one, agree on the partitioning at ambient temperature. However, extrapolation of our results to $T = 220$ K gives a value of $\alpha = 0.81$, indicating a significantly less pronounced temperature dependence of the branching ratio and a different partitioning of the products of the BrO self-reaction at temperatures typical of the Arctic Boundary Layer, as discussed below. However, given the evidence of a termolecular component to the BrO self-reaction at $T < 250$ K (at the concentrations used in this and other laboratory studies), the assumption of a branching ratio based on a two-channel mechanism may be inappropriate, indicating the need for further studies.

The study from Jaffe and Mainquist[7] reports a parameterisation of the temperature dependence of the ratio k_{1a}/k_{1b} from the analysis of bromine photosensitised decomposition of ozone in the range $T = 258$–333 K. Their values of k_{1a}/k_{1b} are obtained from the quantum yields for ozone decomposition based on the assumption that Br atoms are in steady state. The branching ratio for channel (1a) is related to k_{1a}/k_{1b} *via*:

$$\alpha = \frac{k_{1a}}{k_1} = \left[1 + \left(\frac{k_{1a}}{k_{1b}}\right)^{-1}\right]^{-1} \qquad \text{(x)}$$

Values for α were calculated from Jaffe and Mainquist's k_{1a}/k_{1b} using eqn (x) and are shown in Fig. 7. They agree well with the branching ratios measured in this work and with those recorded by Cox *et al.*[12]

The values of k_1 from this study are higher than those reported by Sander and Watson,[8] Turnipseed *et al.*[13] and Harwood *et al.*[21] Data from Sander and Watson were recorded at three temperatures between $T = 223$ K and $T = 388$ K, data from Turnipseed *et al.* at three temperatures over the range $T = 253$–400 K, data from Harwood *et al.* at three temperatures in the range $T = 250$–298 K. Harwood *et al.* recorded data at two temperatures below 250 K; however, since the same authors observed that Arrhenius behaviour is lost below 250 K, these two data points have been excluded from this discussion. The temperature dependence from Sander and Watson only relies on three points, one of which lies below $T = 250$ K: the authors observed no pressure dependence at $T = 223$ K, whereas both Mauldin *et al.* and Harwood *et al.* reported pressure-dependent rate constants at very similar temperatures ($T = 220$ K and $T = 222$ K respectively). The temperature dependences observed by both Harwood *et al.* and Turnipseed *et al.* also carry noteworthy statistical uncertainty since they rely on three temperature measurements only.

On the other hand, the current study measured the kinetic parameters of both channels at nine temperatures and it is similar in extent to the work of Gilles *et al.*,[19] whose values of k_1 are in very good agreement with those reported here. Gilles *et al.* studied the BrO self-reaction at nine temperatures but over a much broader T range ($T = 204$–388 K). The narrower temperature range used this in work ($T = 265.5$–320.6 K) was

dictated by several reasons: Harwood *et al.* observed pressure-dependent rate constants below 250 K and attributed the deviation from linear Arrhenius behaviour to the termolecular association channel leading to the dimerisation of BrO. To avoid the onset of potential complicating non-bimolecular BrO decay and to avoid condensation of Br_2 in the reactive mixture (melting point of bromine: 265.8 K), T = 265.5 K was chosen as the lowest temperature. The upper temperature limit was dictated by limitations of the thermostatting unit set-up.

Since the second-order nature of BrO decay gave rate constants dependent upon absolute concentrations, and hence absorption, of BrO radicals, discussion of the BrO cross-section employed in previous studies[5,8,21] where BrO was monitored using UV absorption spectroscopy is necessary. Both Harwood *et al.*[21] and Mauldin *et al.*[5] used the BrO cross-section measured by Wahner *et al.*[26] Direct comparison of the σ_{BrO} measured by Wahner *et al.* and Wilmouth *et al.*,[6] whose cross-section was used in the present work, is possible as both reported σ_{BrO} at a spectral resolution of 0.40 nm FWHM. Wahner *et al.* report a value for σ_{BrO} at the (7,0) vibronic peak (λ = 338.5 nm) of 1.55×10^{-17} cm^2 molecule^{-1}, whereas Wilmouth *et al.* measured a very slightly higher cross-section of 1.58×10^{-17} cm^2 molecule^{-1} for the same spectral band.

Accounting for the different cross-sections on second-order kinetic studies allows scaling of correct kinetic parameters to equivalent cross-sections. The values of k_1 reported by Harwood *et al.* and by Mauldin *et al.* are respectively *ca.* 14% and 18% lower than k_1 from this work at T = 298 K. When scaled up to the cross-section from Wilmouth *et al.*, these values are very slightly different, and respectively 13% and 16% lower than k_1 from this work.

Sander and Watson[8] measured the BrO cross-section at the (7, 0) band at all experimental temperatures (T = 223, 298 and 388 K) at a resolution of 0.09 nm FWHM. Their value of σ_{BrO} at T = 298 K is $(1.14 \pm 0.14) \times 10^{-17}$ cm^2 molecule^{-1}, lower than the ones reported by both Wahner *et al.*,[25] $(1.55 \pm 0.13) \times 10^{-17}$ cm^2 molecule^{-1}, and by Wilmouth *et al.*,[6] 1.58×10^{-17} cm^2 molecule^{-1}, both reported at a lower resolution (0.4 nm FWHM). This is unexpected since, as the peaks of structured spectra become sharper at higher resolution, the cross-section reported by Sander and Watson might be expected to exceed those measured by Wahner *et al.* and Wilmouth *et al.* at lower resolutions. Both Wahner *et al.* and Gilles *et al.* argue that Sander and Watson did not actually measure σ_{BrO} at the peak of the (7, 0) band, which is reported at λ = 338.5 nm: Sander and Watson measured the BrO cross-section at λ = 339 nm, hence missing the peak and recording a noticeably lower BrO cross-section. For comparison purposes, σ_{BrO} at λ = 339 nm reported by Wilmouth *et al.* (obtained from the reported spectrum) is 1.27×10^{-17} cm^2 molecule^{-1}, in good agreement with Sander and Watson despite the lower resolution (which affects the tails of spectral peaks to a lesser extent than the peak itself). The same comparison holds for the other two temperatures reported by Sander and Watson: at T = 223 K, they measured $\sigma_{BrO} = (1.56 \pm 0.14) \times 10^{-17}$ cm^2 molecule^{-1} (*cf.* 1.47×10^{-17} cm^2 molecule^{-1} at λ = 339 nm, interpolated from Wilmouth *et al.*) and at T = 388 K, they measured $\sigma_{BrO} = (0.96 \pm 0.12) \times 10^{-17}$ cm^2 molecule^{-1} (*cf.* 1.02×10^{-17} cm^2 molecule^{-1} at λ = 339 nm, interpolated from Wilmouth *et al.*).

The BrO cross-section determined by Gilles *et al.*[19] at a resolution of 0.5 nm FWHM for the (7,0) band (1.63×10^{-17} cm^2 molecule^{-1}) is in good agreement with that of Wilmouth *et al.*[6] degraded to the lower resolution (1.56×10^{-17} cm^2 molecule^{-1}). k_1 reported by Gilles *et al.* is 3.6% higher than the one from this work at T = 298 K; after scaling to the cross-section used in this work, they agree within 0.8%.

Turnipseed *et al.*[13] measured k_1 using discharge flow coupled with mass spectrometry. Their method therefore did not rely on the determination of the BrO cross-section. They obtained two values for k_1, one from O + Br_2 and one from Br + O_3. These values of k_1 at T = 304 K are respectively *ca.* 31% and 34% lower than interpolation from the results of the present study to the same temperature. The reason for this discrepancy remains uncertain.

4.3 Sensitivity analysis

Sensitivity to uncertainties in the absorption cross-section of BrO from Wilmouth *et al.*[6] was also taken into account. These authors report an error of ±11% for the differential cross-section of the (7, 0) band (λ = 338.5 nm) at T = 298 K. A sample [BrO] trace at T = 298 K was therefore perturbed by a factor of 11% and fit to the FACSIMILE model. The values of k_{1a} and k_{1b} obtained from the fit to the perturbed traces were within respectively 25% and 10% of the values resulting from fitting to the unperturbed traces.

Sensitivity studies were also undertaken to ascertain effective masking of channel (1a) under our experimental conditions and to assess the effect of secondary chemistry.

A FACSIMILE[27] model of the BrO self-reaction was developed including reactions (1a), (1b) and (2) and sensitivity of the BrO decay to channel (1a) was tested for different ozone concentrations. The optimal ozone concentration in the precursor mixture had to be high enough to ensure prompt conversion of Br atoms produced by channel (1a) into BrO *via* reaction (2); however, the higher the concentration of ozone, the poorer the signal due to the large absorption cross-section of O_3, and therefore weaker signal, in the near-UV. Sensitivity of the BrO decay to channel (1a) at different [O_3] was tested by perturbing k_{1a} by a factor of two and refitting the simulated decay to extract the overall rate constant. It was found that, at ozone concentrations of (1–2) $\times 10^{16}$ molecules cm^{-3}, as used in this work, the overall BrO decay was independent of k_{1a} and depended solely on k_{1b}.

Rowley *et al.*[17] observed Br_2O formation at relatively high [BrO]/[O_3] ratios ($> 10^{-3}$) *via* reaction (4):

$$Br + BrO + M \rightarrow Br_2O + M \qquad (4)$$

Since the [BrO]/[O_3] ratio in this work fluctuated between (2–6) $\times 10^{-3}$, contribution of reaction (4) to the observed BrO decay had to be taken into account. FACSIMILE simulations were run including reaction (4) in the kinetic model, with rate constant expressed as $k_4 = 1.9 \times 10^{-14} \exp(1370/T)$ as

determined by Harwood *et al.*[21] Simulations showed that, at the precursor concentrations used in the present work, [Br_2O] reached a maximum concentration over the timescale of the experiments of approximately 3×10^{11} molecules cm^{-3} at $T = 298$ K and 5×10^{11} molecules cm^{-3} at $T = 265.55$ K, two orders of magnitude smaller than the observed BrO concentrations.

BrO traces were also simulated using two FACSIMILE models: one excluding and one including reaction (4). The simulated BrO decays were then fitted to the standard solution for $-d[BrO]/dt$, eqn (vi). The values of k_{1b} extracted from the trace simulated with the inclusion of reaction (4) were 0.7% and 1.2% higher than the ones obtained from the model without reaction (4) at $T = 298$ K and $T = 265.5$ K respectively. Moreover, the Br_2O spectrum exhibits a peak at $\lambda = 312$ nm of 2.22×10^{-18} cm^2 $molecule^{-1}$,[23] and no appreciable evidence for Br_2O absorbance was found after spectral subtraction of the BrO and O_3 contributions to the recorded spectra (Fig. 1).

OBrO formation *via*:

$$BrO + O_3 \rightarrow OBrO + O_2 \qquad (5)$$

was observed by Rowley *et al.*[17] at very low [BrO]/[O_3] ratios ($<10^{-4}$). This ratio is too low compared to that resulting from the concentrations used in this work: ozone concentrations in the order of at least 10^{17} molecules cm^{-3} are necessary for reaction (5) to effectively compete with reaction (1).

Harwood *et al.*[21] observed pressure dependence of the overall rate constant k_1 at temperatures lower than 250 K. This behaviour was attributed to the BrO dimerisation reaction, analogous to the ClO dimerisation reaction:[28]

$$BrO + BrO + M \leftrightarrows Br_2O_2 + M \qquad (6,-6)$$

As the lowest temperature in the present study is $T = 265.5$ K, it is highly unlikely for reactions (6,−6) to occur, on the basis of previous studies.

4.4 Atmospheric implications

Despite being of minor significance in the stratosphere due to low BrO mixing ratios, the BrO self-reaction is very important in the troposphere, especially in the Arctic Marine Boundary Layer during springtime, when BrO concentrations are relatively high. This work measured a significantly weaker temperature dependence of the partitioning of channels (1a) and (1b) than the current JPL-NASA[23] recommendation. Our findings imply that channel (1a), which directly depletes ozone, dominates the branching of reaction (1) at temperatures typical of the Arctic Boundary Layer to a greater extent than currently thought. Therefore the partitioning between active (Br) and inactive bromine (Br_2) could be shifted towards the former, leading to a potential increased ozone-depleting efficiency of the BrO catalytic cycle.

5. Conclusion

The BrO self-reaction has been characterised as a function of temperature in the lower tropospheric regime. Arrhenius expressions for both channels and for the overall reaction (1) were derived. The temperature dependence of the extrapolated overall rate of reaction (1) is in good agreement with the current JPL-NASA recommendation;[23] they agree within 6% at $T = 250$ K. However the branching of the BrO self-reaction determined in this work shows a weaker temperature dependence than previously determined with implications for the ozone-depleting efficiency of the BrO self-reaction in regions such as the Polar Boundary Layer.

References

1 P. A. Newman, M. Rex, (Lead Authors); P. O. Canziani, K. S. Carslaw, K. Drdla, S. Godin-Beekmann, D. M. Golden, C. H. Jackman, K. Kreher, U. Langematz, R. Müller, H. Nakane, Y. J. Orsolini, R. J. Salawitch, M. L. Santee, M. von Hobe, S. Yoden, *Polar Ozone*: *Past and Present*, Chapter 4 in *Scientific Assessment of Ozone Depletion*: *2006*, *Global Ozone Research and Monitoring Project*-Report No. 50, 572 pp., World Meteorological Organization, Geneva, Switzerland, 2007.
2 M. Hausmann and U. Platt, *J. Geophys. Res.*, 1994, **99**(D12), 25399.
3 U. Platt and G. Hönninger, *Chemosphere*, 2003, **52**, 325.
4 Y. Bedjanian and G. Poulet, *Chem. Rev.*, 2003, **103**, 4639.
5 R. L. Mauldin III, A. Wahner and A. R. Ravishankara, *J. Phys. Chem.*, 1993, **97**, 7585.
6 D. M. Wilmouth, T. F. Hanisco, N. M. Donahue and J. G. Anderson, *J. Phys. Chem. A*, 1999, **103**, 8935.
7 S. Jaffe and W. K. Mainquist, *J. Phys. Chem.*, 1980, **84**, 3277.
8 S. P. Sander and R. T. Watson, *J. Phys. Chem.*, 1981, **85**, 4000.
9 M. A. A. Clyne and H. W. Cruse, *Trans. Faraday Soc.*, 1970, **66**, 2214.
10 N. Basco and S. K. Dogra, *Proc. R. Soc. London, Ser. A*, 1971, **323**, 417.
11 M. A. A. Clyne and R. T. J. Watson, *J. Chem. Soc., Faraday Trans. 1*, 1975, **71**, 336.
12 R. A. Cox, D. W. Sheppard and M. P. Stevens, *J. Photochem.*, 1982, **19**, 189.
13 A. A. Turnipseed, J. W. Birks and J. G. Calvert, *J. Phys. Chem.*, 1991, **95**, 4356.
14 I. T. Lançar, G. Laverdet, G. LeBras and G. Poulet, *Int. J. Chem. Kinet.*, 1991, **23**, 37.
15 I. Bridier, B. Veyret and R. Lesclaux, *Chem. Phys. Lett.*, 1993, **201**, 563.
16 O. V. Rattigan, R. A. Cox and R. L. Jones, *Chem. Phys. Lett.*, 1994, **230**, 121.
17 D. M. Rowley, M. H. Harwood, R. A. Freshwater and R. L. Jones, *J. Phys. Chem.*, 1996, **100**, 3020.
18 B. Laszlo, R. E. Huie and M. J. Kurylo, *J. Geophys. Chem.*, 1997, **102**, 1523.
19 M. K. Gilles, A. A. Turnipseed, J. B. Burkholder, A. R. Ravishankara and S. Solomon, *J. Phys. Chem. A*, 1997, **101**, 5526.
20 Y. Bedjanian, G. LeBras and G. Poulet, *J. Phys. Chem. A*, 1998, **102**, 10501.
21 M. H. Harwood, D. M. Rowley, R. A. Cox and R. L. Jones, *J. Phys. Chem. A*, 1998, **102**, 1790.
22 R. Atkinson, D. L. Baulch, R. A. Cox, J. N. Crowley, R. F. Hampson, R. G. Hynes, M. E. Jenkin, M. J. Rossi and J. Troe, Evaluated kinetic and photochemical data for atmospheric chemistry: Volume III—gas phase reactions of inorganic halogens, *Atmos. Chem. Phys.*, 2007, **7**, 981.
23 S. P. Sander, B. J. Finlayson-Pitts, R. R. Friedl, D. M. Golden, R. E. Huie, H. Keller-Rudek, C. E. Kolb, M. J. Kurylo, M. J. Molina, G. K. Moortgat, V. L. Orkin, A. R. Ravishankara and P. H. Wine, *Chemical Kinetics and Photochemical Data for Use in Atmospheric*

Studies, JPL Publication 06-2, NASA Jet Propulsion Laboratory, Pasadena, 2006.
24 G. Boakes, W. H. Hindi Mok and D. M. Rowley, *Phys. Chem. Chem. Phys.*, 2005, **7**, 4102.
25 V. Ferracci and D. M. Rowley, *Phys. Chem. Chem. Phys.*, 2010, **12**, 11596.
26 A. Wahner, A. R. Ravishankara, S. P. Sander and R. R. Friedl, *Chem. Phys. Lett.*, 1988, **152**, 507.
27 A. R. Curtis and W. P. Sweetenhan, *FACSIMILE*, AERE Harwell Publication, Oxford, 1987.
28 L. T. Molina and M. J. Molina, *J. Phys. Chem.*, 1987, **91**, 433.